



ELSEVIER

Available online at [www.sciencedirect.com](http://www.sciencedirect.com)

SCIENCE @ DIRECT®

Nuclear Instruments and Methods in Physics Research B 205 (2003) 399–404

NIM B  
Beam Interactions  
with Materials & Atoms[www.elsevier.com/locate/nimb](http://www.elsevier.com/locate/nimb)

# Ionization–excitation magnetic sublevel cross sections for $\text{He}^+ (2p)^2\text{P}^0$ states following fast electron and proton impact

H. Merabet <sup>a,\*</sup>, R. Bruch <sup>a</sup>, S. Fülling <sup>a</sup>, M. Bailey <sup>a</sup>, A.L. Godunov <sup>b</sup>,  
J.H. McGuire <sup>b</sup>, A.N. Grum-Grzhimailo <sup>c,1</sup>, K. Bartschat <sup>d,2</sup>

<sup>a</sup> Department of Physics, University of Nevada Reno, Reno, NV 89557, USA

<sup>b</sup> Department of Physics, Tulane University, New Orleans, LA 70118, USA

<sup>c</sup> Department of Physics and Astronomy, Drake University, Des Moines, IA 50311, USA

<sup>d</sup> ITAMP, Harvard Smithsonian Center for Astrophysics, Cambridge, MA 02138, USA

## Abstract

The first experimental magnetic substate scattering-angle-integrated cross sections following ionization–excitation of  $\text{He}(1s^2) ^1\text{S}$  to  $\text{He}^+(2p)^2\text{P}^0$  in the  $e^- + \text{He}$  collision system have been determined using a combination of total cross sections and polarization fraction measurements in the extreme ultraviolet range. The derived magnetic sublevel cross sections,  $\sigma_0$  and  $\sigma_1$ , for  $M_L = 0, \pm 1$  have been studied over a wide range of electron velocities (2–8.5 a.u.). These results are compared with previous cross sections for equi-velocity proton impact. In addition, our experimental data are compared with earlier theoretical predictions, our recent second-Born calculations fully including off-energy shell terms, and new R-matrix results. We have extended our polarization measurements for  $\text{H}^+ + \text{He}$  collisions and found excellent agreement between theory and experiment at nearly all impact energies. However, the present second-Born and R-matrix results deviate slightly from the experimental electron data.

© 2003 Elsevier Science B.V. All rights reserved.

PACS: 34.50.Fa; 34.80.Dp

Keywords: Ionization–excitation; Sublevel cross sections; Electron impact; Proton impact; Helium

## 1. Introduction

Two-electron atomic systems are of fundamental importance to the investigation of complex many-body problems in collision physics [1]. In the past, great effort has been devoted to the study of atomic and molecular collisions using helium the atom as a target [2–7]. Indeed, helium as the simplest two-electron system is perfectly suited for studying time ordering, including both static and

\* Corresponding author. Tel.: +1-775-784-1335; fax: +1-775-784-1398.

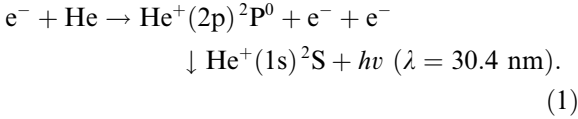
E-mail address: [hocine@physics.unr.edu](mailto:hocine@physics.unr.edu) (H. Merabet).

<sup>1</sup> Permanent address: Institute of Nuclear Physics, Moscow State University, 119992 Moscow, Russia.

<sup>2</sup> Permanent address: Department of Physics and Astronomy, Drake University, Des Moines, IA 50311, USA.

dynamic electron correlation [1,8–10]. Recently simultaneous ionization–excitation by electron and proton impact has attracted much attention both theoretically and experimentally [1–19]. However, experimental data still show systematic deviations from the most sophisticated theoretical calculations presently available.

In the present work we investigate the simultaneous ionization–excitation from the  $\text{He}(1s^2)^1\text{S}$  ground state to the final ionic state  $\text{He}^+(2p)^2\text{P}^0$  (also noted as  $\text{HeII}(2p)^2\text{P}^0$ ) in  $e^- + \text{He}$  single collisions, followed by short wavelength radiative decay to the  $\text{He}^+(1s)^2\text{S}$  as follows:



This process is difficult to investigate, experimentally due to very small extreme ultraviolet (EUV) emission cross sections, and theoretically because the electrons of the target are highly correlated.

We have measured total cross sections  $\sigma$  for the  $\text{He}^+(2p)^2\text{P}^0$  state following electron and proton impact on helium using EUV spectrometry [7]. We note that these absolute total cross sections do not provide direct information about the magnetic substate populations, while linear polarization measurements yield only the magnetic sublevel cross section ratios  $\sigma_0/\sigma_1$ . Such ratios are directly related to the degree of linear polarization (20) as

$$P = \frac{I_{\parallel} - I_{\perp}}{I_{\parallel} + I_{\perp}} = \frac{3(\sigma_0 - \sigma_1)}{7\sigma_0 + 11\sigma_1} = \frac{3(r - 1)}{7r + 11}, \quad (2)$$

where  $I_{\parallel}$  is the intensity of radiation with electric field vectors oriented along the beam axis and  $I_{\perp}$  is the intensity of radiation with a transverse electric field vector (perpendicular to the plane formed by the incident projectile beam and the direction of observation);  $r = \sigma_0/\sigma_1$ , is the cross section ratio. Moreover, the total cross section  $\sigma$  is the sum of the three magnetic sublevel angle-integrated cross sections,

$$\sigma = \sigma_0 + 2\sigma_1. \quad (3)$$

Thus, by combining Eqs. (2) and (3), the magnetic sublevel cross sections can be obtained.

In this paper, we have combined measurements of two experimental techniques, namely EUV

spectrometry and EUV polarimetry, to determine the first experimental sublevel cross section results for  $\text{He}^+(2p)^2\text{P}^0$  states following electron impact at a wide range of projectile velocities ( $2 < v < 8.5$  a.u.). In addition, we have extended polarization proton measurements to include more collisions velocities. This allowed us to make a comprehensive comparison for negatively and positively singly charged projectiles. The experimental data are also compared with our most recent first- and second-order Born calculations including on- and off-shell terms [10,12] along with different theoretical predictions for electron and proton impacts [11,16,17].

## 2. Results and discussion

The experimental setup used in this work consists of three main components: an EUV polarimeter; an electron gun or a 2 MV Van de Graaff accelerator, target cell and Faraday cup; and a 1.5 m grazing incidence monochromator. A PC controlled data acquisition system has been used to operate the apparatus and to record the data. A complete description of this experimental setup is given by Merabet et al. [7,20]. In brief, the polarimeter utilizes a molybdenum–silicon (Mo/Si) MLM optimized a wavelengths  $\lambda = 304 \text{ \AA}$  at an incidence angle of  $50^\circ$ , corresponding to the  $\text{HeII}(2p)^2\text{P}^0 \rightarrow (1s)^2\text{S}$  transition. Our polarization measurements have been performed with a 10% VYNS spectral filter [4,5] that provides a transmission ratio of HeI/HeII line intensities of approximately 1000 000:1. In fact, the polarization measured with this filter contained approximately only a 1% contribution from the dominating  $\text{HeI}(1snp)^1\text{P}^0$  radiative emission. The corresponding total cross sections  $\sigma$  measurements have been conducted using a 1.5 m high resolution grazing incidence monochromator [7,12,20]. A detailed pressure dependence of the emission from ionized–excited helium was obtained both with the 1.5 m grazing incidence monochromator and the EUV polarimeter. To ensure single collision conditions for the Lyman- $\alpha$  of HeII line a target pressure of 1 mTorr was selected. The gas cell used in this study was mounted inside a cylindrical magnetic shielding in order to avoid depolariza-

tion due to magnetic fields (Hanle effect). With this shielding at the interaction region of the gas target a magnetic field smaller than 0.05 G was achieved. The proton results have been put on the absolute scale by renormalizing our proton data [12] to full second-Born cross section values for high velocities impact ( $v = 6.1$  a.u.). Then, electron cross sections were normalized to proton measurements by keeping the same electron to proton cross section ratios for equi-velocity projectile impact. In addition, the obtained cross section data have been corrected for alignment effects using [21]

$$\sigma(\theta) = \sigma \times \{1 + A_0 P_2(\cos \theta)\}, \quad (4)$$

where  $\sigma(\theta)$  is the measured cross section,  $\theta = 90^\circ$  is the observation angle of the emitted photons,  $\sigma$  is the cross section for an isotropic distribution,  $P_2(\cos \theta)$  is the second Legendre polynomial and  $A_0$  is the alignment parameter that is related to the degree of linear polarization by [20]

$$P(^2P^0) = \frac{3A_0}{A_0 - 6}. \quad (5)$$

The statistical uncertainties of the measured line intensities in this study were between 0.5% and 1% over most of the range of impact energies. When instrumental uncertainties related to energy resolution of the Van de Graaff accelerator, target pressure stability, polarization and charge normalization are combined, the total uncertainty for magnetic scattering-angle-integrated substate cross sections was found to be about 12–15% for HeII(2p)<sup>2</sup>P<sup>0</sup> states. The current experimental HeII(2p)<sup>2</sup>P<sup>0</sup> polarization results have not been corrected for cascade effects because the partial magnetic substate cross sections for the higher HeII( $n\ell$ ) magnetic sub-states are not yet accurately known.

Using Eqs. (2) and (3), we have derived  $\sigma_M$  following the He<sup>+</sup>(2p)<sup>2</sup>P<sup>0</sup> → (1s)<sup>2</sup>S transition in e<sup>-</sup> + He and H<sup>+</sup> + He collisions at impact energies ranging from 80 to 980 eV ( $2 < v_e < 8.5$  a.u.) and 100–916 keV ( $2 < v_p < 6.1$  a.u.), respectively. The first- and second-Born calculations results presented in this work for electrons are obtained using the same theoretical approach as for previous proton calculations [12]. More details about these calculations are given elsewhere [10].

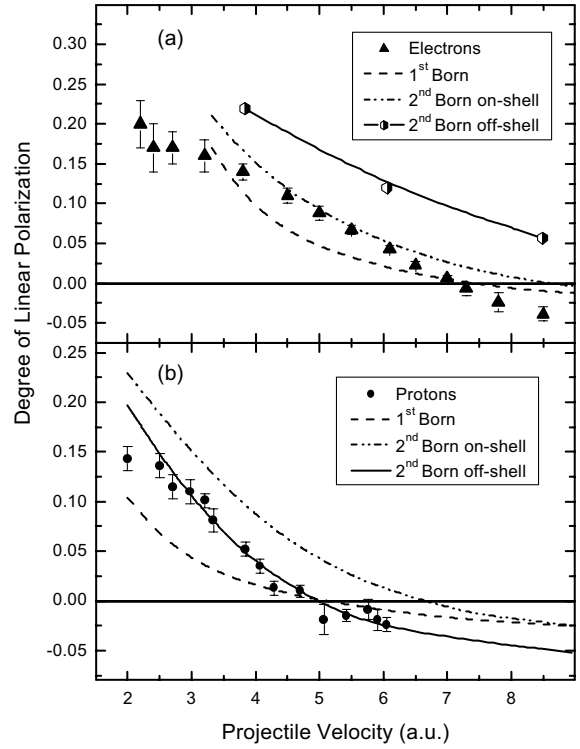


Fig. 1. Degree of linear polarization following helium EUV emission as function of electron and protons velocity compared with first- and second-Born calculations.

We have plotted in Fig. 1 the degree of linear polarization for the emitted EUV radiation following electron and proton impact along with first-Born, approximate second-Born including only spatial correlation (second-Born on-shell), and the full second-Born calculations (second-Born off-shell), which account for both spatial and temporal correlations. The off-shell energy terms represent time correlation between the two-active electrons. Fig. 1(b) exhibits an excellent convergence of the full second-Born calculations towards the experiment for protons whereas this is not the case for electron impact (Fig. 1(a)), where the agreement is less favorable. The electron-impact second-order calculations are more sensitive to the quality and number of the intermediate states and this may explain such deviations in our calculations. Therefore, more theoretical investigations with a better target description are envisaged in the near future.

Fig. 2 shows the observed  $\text{He}^+(2p)^2\text{P}^0$  total cross sections compared with Born predictions as well as other theoretical calculations for electrons and protons. These experimental data are obtained by renormalizing our previous results of Bailey et al. [5] and those of Forand et al. [2] to the second Born including off-shell terms for protons [12]. It is clear from this figure that the full second-Born calculations reproduce very well the proton data over the entire velocity range investigated while the ionization–excitation cross sections calculated with the impact-parameter method and second-order perturbations (Nagy and Benedek [11]) converge towards our experimental findings in the 4–6 a.u. velocity range but fail to match them at lower impact velocities. Nonetheless, the difference between these theoretical results and our experiment is less than 40%. This discrepancy is by far

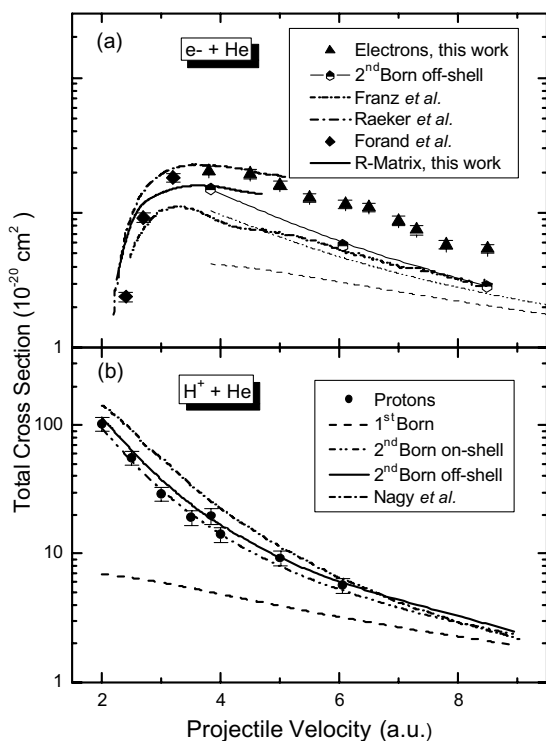


Fig. 2. Total cross sections for ionization–excitation to  $\text{He}^+(2p)^2\text{P}^0$  states by electron and proton impact. Notations are the same as Fig. 1 unless indicated otherwise. The Forand experimental data indicated here are renormalized (see text). The calculations of Nagy and Benedek are from [11].

smaller than prior disagreement between theory and experiment.

We also show in Fig. 2(a) earlier theoretical total cross sections for electron impact on helium; namely, second-Born results of Franz and Altick [17] and R-matrix calculations of Raeker et al. [16] together with our renormalized data, first and second Born, as well as our present 23-state R-matrix predictions. The R-matrix models treat the interaction of a fast electron with the target by a first-order distorted-wave model, while the initial state and the ejected-electron–residual-ion interaction are described by a close-coupling expansion. Although the 6-state results of Raeker et al. seem to be in excellent agreement with our measurements in the 3–5 a.u. velocity range, this agreement is likely accidental since improving the model actually decreases the predicted cross sections, resulting in poorer agreement with experiment. More accurate R-matrix calculations,

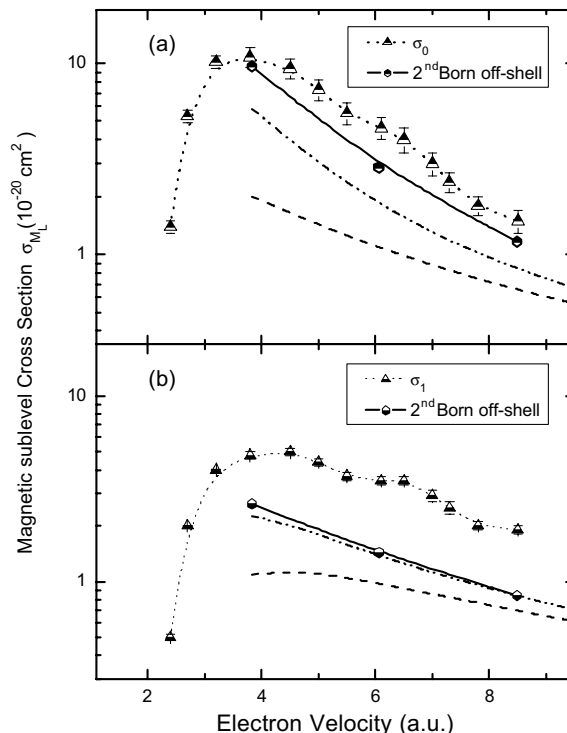


Fig. 3. Magnetic sublevel cross sections  $\sigma_0$  and  $\sigma_1$  for electron impact on helium. Notations are the same as Fig. 1 unless indicated otherwise.

including second-order effects, are currently being performed. We note that the second-Born off-shell total cross sections coincide with the 23-state first-order R-matrix results at the lowest velocity. On the other hand, the total cross sections of Franz et al. are consistent with our full second-Born results at high impact energies and nicely reproduce the experimental data at low impact velocities.

The sublevel cross sections  $\sigma_0$  and  $\sigma_{\pm 1}$  for HeII(2p)<sup>2</sup>P<sup>0</sup> states for electron impact are depicted in Fig. 3 and compared with our present Born calculations for impact velocities  $v \geq 3.8$  a.u. since at lower energies higher-order terms beyond second-order are expected to be significant [10]. The behavior of the  $\sigma_0$  and  $\sigma_{\pm 1}$  cross sections is qualitatively similar to the total cross section for excitation-ionization. The first-Born cross sections and experimental data do not converge in the in-

vestigated velocity range. The second-Born effect including off-shell terms increases the first-Born cross sections and therefore improves agreement with the EUV measurements. Such convergence is good for  $\sigma_0$  but still not satisfactory for  $\sigma_{\pm 1}$ . This confirms that the independent-time approximation (2) is more sensible for the  $M_L = \pm 1$  magnetic substate population  $\sigma_{\pm 1}$  than for  $\sigma_0$  [12].

As a preliminary investigation of the ionization–excitation process for positively and negatively singly charged projectiles, we have examined the dependence of the polarization fraction as well as the total and sublevel cross sections for electron and proton impact. Fig. 4 exhibits a comparison of these observables. It is evident that the degree of linear polarization behaves differently for electrons and protons (see Fig. 4(a)), suggesting a less pronounced anisotropy of the emitted radiation.

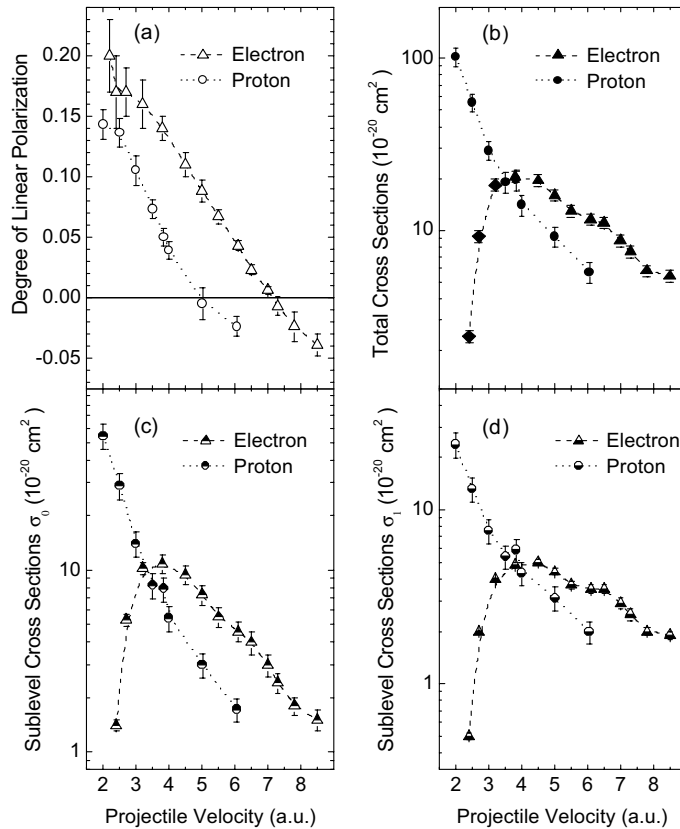


Fig. 4. Experimental polarization fraction, total and sublevel cross sections as a function of projectile velocities compared for electron and proton impact. Curves are provided to guide the eye.

We note that the general trend for all measured cross sections following electron impact shows a steep increase in cross section for small impact velocities, reaching a maximum around 4 a.u. Then follows a gradual decrease with increasing electron velocity towards the asymptotic high energy limit. However, significant differences between electron and proton impact occur over the entire energy range investigated. In particular it is observed that the cross sections for the proton impact are larger than those obtained for electron impact at lower velocities ( $v < 4$  a.u.). Then they continue to decrease as the impact velocity increases and become smaller than the electron cross sections at higher proton energies.

In summary, based upon excellent agreement between theory and experiment for the sublevel cross section ratios determined under identical experimental conditions for proton impact on helium, we propose newly normalized total cross sections that may overcome the factor 2 or 3 deviation between various theoretical predictions and previous electron-impact measurements. Furthermore, we have presented the first measured angle-integrated sublevel cross sections for e–He ionization–excitation. A preliminary comparison of these quantities for electron and proton impact is also presented for equivalent velocities impact, along with recent and earlier theoretical calculations. Only modest agreement is found between our theoretical results and the experimental data for electron impact, suggesting the need for more sophisticated treatments of the target description and/or the inclusion of higher-order terms. These findings lend support to the new normalization procedure suggested by Merabet et al. [12] since agreement is nearly reached between experiment and theory for  $e^- + \text{He}$  and  $\text{H}^+ + \text{He}$  scattering. However, a final conclusion on this matter may need additional measurements with better EUV filters than those used by Forand et al.

### Acknowledgements

This project has been supported, in part, by ACSPECT Corp. and the Nevada Business and Science Foundation, (NBSF) Reno, Nevada. K.B.

and A.N.G. acknowledge support from the National Science Foundation under grant PHY-0088917 and by NATO under grant PST.CLG.976837. K.B. was also partially supported by the NSF through a grant for the Institute of Theoretical Atomic and Molecular Physics at Harvard University and the Smithsonian Astrophysical Observatory.

### References

- [1] J.H. McGuire, *Electron Correlation Dynamics in Atomic Collisions*, Cambridge University Press, 1997.
- [2] J.L. Forand, K. Becker, J.W. McConkey, *J. Phys. B* 18 (1985) 1409.
- [3] J.O. Pedersen, F. Folkmann, *J. Phys. B* 23 (1990) 441.
- [4] R. Bruch, E. Rauscher, S. Fülling, *Encyc. Appl. Phys.* 10 (1994) 437.
- [5] M. Bailey, R. Bruch, E. Rauscher, S. Bliman, *J. Phys. B* 28 (1995) 2655.
- [6] W. Stolte, R. Bruch, *Phys. Rev. A* 54 (1996) 2166.
- [7] H. Merabet, M. Bailey, R. Bruch, J. Hanni, S. Bliman, D.V. Fursa, I. Bray, K. Bartschat, H.C. Tseng, C.D. Lin, *Phys. Rev. A* 64 (2001) 012712.
- [8] A.L. Godunov, J.H. McGuire, *J. Phys. B* 34 (2001) L223.
- [9] J.H. McGuire, A.L. Godunov, S.G. Tolmanov, Kh. Shakov, R. Dörner, H. Schmidt-Böcking, R.M. Dreizler, *Phys. Rev. A* 65 (2001) 052706.
- [10] A.L. Godunov, J.H. McGuire, P.B. Ivanov, V.A. Shipakov, H. Merabet, R. Bruch, J. Hann, Kh. Shakov, *J. Phys. B* 34 (2001) 5055.
- [11] L. Nagy, Á. Benedek, *J. Phys. B* 35 (2002) 491.
- [12] H. Merabet, R. Bruch, J. Hanni, A.L. Godunov, J.H. McGuire, *Phys. Rev. A* 65 (2002) R010703.
- [13] Y. Fang, K. Bartschat, *J. Phys. B* 34 (2001) L19.
- [14] P.J. Marchalant, B. Rouvellou, J. Rasch, S. Rioual, C.T. Whelan, A. Pochat, D.H. Madison, H.R.J. Walters, *J. Phys. B* 33 (2000) L749.
- [15] M.R.H. Rudge, *J. Phys. B* 21 (1988) 1887.
- [16] A. Raeker, K. Bartschat, R.H.G. Reid, *J. Phys. B* 27 (1994) 3129.
- [17] A. Franz, P. Altick, *J. Phys. B* 28 (1995) 4639.
- [18] L. Nagy, J. Wang, J.C. Straton, J.H. McGuire, *Phys. Rev. A* 52 (1995) R902.
- [19] B. Rouvellou, S. Rioual, A. Pochat, R.J. Tweed, J. Langlois, G. Nguyen Vien, O. Robaux, *J. Phys. B* 33 (2000) L599.
- [20] H. Merabet, M. Bailey, R. Bruch, D.V. Fursa, I. Bray, J.W. McConkey, P. Hammond, *Phys. Rev. A* 60 (1999) 1187.
- [21] A. Götz, W. Mehlhorn, A. Raeker, K. Bartschat, *J. Phys. B* 29 (1996) 4699.